

Widespread extrahippocampal NAA/(Cr+Cho) abnormalities in TLE with and without mesial temporal sclerosis

Susanne G. Mueller · Andreas Ebel · Jerome Barakos ·
Cathy Scanlon · Ian Cheong · Daniel Finlay · Paul Garcia ·
Michael W. Weiner · Kenneth D. Laxer

Received: 26 July 2010/Revised: 29 September 2010/Accepted: 7 October 2010/Published online: 26 October 2010
© The Author(s) 2010. This article is published with open access at Springerlink.com

Abstract MR spectroscopy has demonstrated extrahippocampal NAA/(Cr+Cho) reductions in medial temporal lobe epilepsy with (TLE-MTS) and without (TLE-no) mesial temporal sclerosis. Because of the limited brain coverage of those previous studies, it was, however, not possible to assess differences in the distribution and extent of these abnormalities between TLE-MTS and TLE-no. This study used a 3D whole brain echoplanar spectroscopic imaging (EPSI) sequence to address the following questions: (1) Do TLE-MTS and TLE-no differ regarding severity and distribution of extrahippocampal NAA/(Cr+Cho) reductions? (2) Do extrahippocampal NAA/(Cr+Cho) reductions provide additional information for focus lateralization? Forty-three subjects (12 TLE-MTS, 13 TLE-no, 18 controls) were studied with 3D EPSI. Statistical parametric mapping (SPM2) was used to identify regions of significantly decreased NAA/(Cr+Cho) in TLE groups and in individual patients. TLE-MTS and TLE-no

had widespread extrahippocampal NAA/(Cr+Cho) reductions. NAA/(Cr+Cho) reductions had a bilateral fronto-temporal distribution in TLE-MTS and a more diffuse, less well defined distribution in TLE-no. Extrahippocampal NAA/(Cr+Cho) decreases in the single subject analysis showed a large inter-individual variability and did not provide additional focus lateralizing information. Extrahippocampal NAA/(Cr+Cho) reductions in TLE-MTS and TLE-no are neither focal nor homogeneous. This reduces their value for focus lateralization and suggests a heterogeneous etiology of extrahippocampal spectroscopic metabolic abnormalities in TLE.

Keywords Temporal lobe epilepsy · Mesial temporal sclerosis · NAA · Spectroscopy

Introduction

Temporal lobe epilepsy (TLE) is the most common form of partial epilepsy. Two types of non-lesional medial TLE are distinguished based on imaging and histopathological findings: (1) TLE with mesial temporal lobe sclerosis (TLE-MTS, about 60–70%), which is characterized by an atrophied hippocampus with MR signal abnormalities and severe neuronal loss in the histological examination, and (2) TLE with a normal appearing hippocampus on the MRI (TLE-no, about 30–40%) and no or mild neuronal loss in the histological examination. The differences between the two TLE types, however, are not restricted to the hippocampus and its appearance in the MRI or histopathological preparation. Recent neuroimaging studies have shown that structural and functional abnormalities exist beyond the hippocampus and even beyond the temporal lobe, and that the two groups not only differ regarding severity of these

S. G. Mueller · A. Ebel · C. Scanlon · I. Cheong · D. Finlay ·
M. W. Weiner
Center for Imaging of Neurodegenerative Diseases
and Department of Radiology and Biomedical Imaging,
University of California, San Francisco, CA, USA

J. Barakos · K. D. Laxer
Pacific Epilepsy Program, California Pacific Medical Center,
San Francisco, CA, USA

P. Garcia
Department of Neurology, University of California,
San Francisco, CA, USA

S. G. Mueller (✉)
Department of Veterans Affairs (DVA) Medical Center,
Center for Imaging of Neurodegenerative Diseases,
Clement Street 4150, San Francisco, CA 94121, USA
e-mail: susanne.mueller@ucsf.edu

abnormalities but more importantly also regarding their distribution [1–5]. These findings, together with other crucial clinical differences between TLE-MTS and TLE-no, e.g. history of febrile seizures, age at onset of epilepsy, initial ictal zone [6] or success of epilepsy surgery [7, 8], suggest that TLE-no is more than just a milder form of TLE-MTS but eventually even a distinct entity of TLE.

MR spectroscopy allows the non-invasive measurement of *N*-acetyl-aspartate (NAA) (marker of neuronal viability and functionality), creatine/phosphocreatine (Cr) (marker of energy metabolism), and choline compounds (Cho) (marker of cell membrane integrity), simultaneously and thus provides information about various important aspects of the brain metabolism. The typical spectroscopic hallmark of the epileptogenic focus is an NAA reduction which is generally thought to represent mostly neuron loss [9, 10], while Cho and Cr are unchanged [11]. Using multiple single voxel spectroscopy or multi-slice spectroscopic imaging techniques, it has been shown that NAA reductions are not restricted to the focus in TLE but can be found in extra-hippocampal and extratemporal regions as well [12, 13]. Because of their limited brain coverage, these previous studies were not able to conclusively assess if the distribution and/or extent of these extrafocal NAA reductions differs between TLE-MTS and TLE-no. The recent development of 3D spectroscopic imaging sequences, which provide spectroscopic information from the whole brain, has changed this [14]. Using such a sequence [15] we addressed the following specific aims: (1) Confirm the findings of previous studies showing that extrahippocampal/extratemporal NAA reductions exist in unilateral TLE and to test if TLE-MTS and TLE-no differ regarding the distribution and severity of these abnormalities. Based on recent findings in structural MRI [16], it was assumed that NAA reductions in TLE-MTS would show a mesial-temporal, temporal-posterior to occipital distribution and in TLE-no a temporolateral distribution. (2) Test if severity and extent of extrahippocampal NAA reductions provide additional information for focus lateralization in TLE-MTS or TLE-no. It was assumed that they would be more prominent in the hemisphere and/or lobe containing the epileptogenic focus.

Methods

Study population

The committees of human research at the University of California, San Francisco (UCSF), California Pacific Medical Center, San Francisco (CPMC) and VA Medical Center, San Francisco approved the study, and written informed consent was obtained from each subject according to the Declaration of Helsinki. Twenty-five consecutive patients

suffering from therapy resistant temporal lobe epilepsy with unilateral seizure onset who were evaluated for epilepsy surgery and agreed to undergo the additional special research imaging and spectroscopy protocol at 4 T were recruited between mid 2005 and the end of 2009 from the Pacific Epilepsy Program, CPMC and the Northern California Comprehensive Epilepsy Center, UCSF. Twelve (mean age 39.6 ± 11.5 ; left TLE/right TLE: 7/5, females/males 8/4) had evidence for mesial temporal lobe sclerosis (MTS) on their MRIs (TLE-MTS) and the remaining 13 (mean age 40.5 ± 9.5 ; left TLE/right TLE: 8/5; females/males: 7/6) had normal appearing hippocampi (TLE-no). The findings regarding presence/absence of MTS were confirmed using subfield volumetry in high resolution T2 weighted images [17]. The two groups differed regarding mean age at onset of epilepsy (TLE-MTS: 11.2 ± 10.0 years; TLE-no: 26.2 ± 12.4 years, $p = 0.003$) and mean duration of epilepsy (TLE-MTS: 28.9 ± 15.6 years; TLE-no: 14.8 ± 12.4 years; $p = 0.02$). The identification of the epileptogenic focus was based on seizure semiology and prolonged ictal and interictal Video/EEG/Telemetry (VET) in all patients. In order to qualify as unilateral TLE, all seizures (average 4.8 ± 2.4 /patient) recorded during this time had to be typical for the patient, show EEG features consistent with mesial temporal onset and arise from the same side. All TLE subjects reported having been seizure free for at least 24 h before the 4 T study. The seizure frequency was determined by calculating the mean frequency/month of all seizure types recorded by the patient in the three months before the research MR exam. Table 1 displays the patient characteristics. The control population consisted of 18 healthy age-matched volunteers (mean age 33.5 ± 10.0 ; females/males: 13/5).

MRI acquisition

All studies were performed on a Bruker MedSpec 4T system controlled by a Siemens TrioTM console and equipped with a USA instruments eight channel array coil. The following sequences, which were part of a larger research imaging and spectroscopy protocol, were acquired: (1) volumetric T1-weighted gradient echo MRI (MPRAGE) TR/TE/TI = 2,300/3/950 ms, 7° flip angle, $1.0 \times 1.0 \times 1.0 \text{ mm}^3$ resolution, acquisition time 5 min. (2) 3D echo planar whole brain spectroscopic imaging (EPSI) TR/TE/TI = 1,780/45/280 ms, FOV = $280 \times 280 \times 180 \text{ mm}^3$ (*x, y, z*), spatial matrix: $50 \times 50 \times 18$ points, spectral bandwidth = 1,667 Hz, 800 spectral points. Metabolite and water reference data was acquired in an interleaved fashion with the delay between metabolite and water reference excitations of $\text{TR}_{\text{WR}} = 550$ ms. Total EPSI acquisition time: 27 min. This spectroscopic imaging sequence allows for the detection of the major brain metabolites NAA, Cr and Cho.

Table 1 Patient characteristics

Pat no.	Age/sex	4 T MRI	Focus	Onset	Duration	Risk factors	Histo/outcome
1	35/m	L MTS L temp atrophy	L mesial temp	4	31		L temp/MTS/I/24
2	50/f	L MTS L temp atrophy	L mesial temp	2	49	FS	L temp/MTS/I/6
3	35/f	L MTS	L mesial temp	9	26		L temp/MTS/II/12
4	38/f	L MTS	L mesial temp	6	32	FS	na
5	53/f	L MTS	L mesial temp	28	26	Infection	L temp/MTS/I/6
6	32/f	L MTS	L mesial temp	24	9	Infection	L temp/MTS/IV/6
7	49/f	R MTS	R mesial temp	7	42		R temp/MTS/I/24
8	23/f	R MTS	R mesial temp	5	18	Infection	na
9	33/f	L MTS	L mesial temp	14	20		na
10	63/m	R MTS	R mesial temp	6	58	FS	na
11	32/m	R MTS	R mesial temp	28	4		R temp/MTS/I/9
12	32/m	R MTS, subtle WMH	R mesial temp	1	32	Infection	R temp/MTS/I/4
13	39/m	Small cyst L temp pole	L mesial temp	29	11		na
14	27/f	Normal	L mesial temp	10	17		na
15	33/f	L front WMH	L mesial temp	10	24		L temp/MTS/I/18
16	38/f	Normal	L mesial temp	37	2		na
17	22/f	Normal	R mesial temp	22	0		na
18	45/f	Normal	R mesial temp	31	15		na
19	45/m	WMH	R mesial temp	30	16	Posttrauma	R temp/norm/I/18
20	41/m	Normal	R mesial temp	40	1	Posttrauma	na
21	45/m	Normal	R mesial temp	38	8		na
22	57/m	Normal	L mesial temp	13	44		na
23	53/f	Normal	L mesial temp	47	6		na
24	42/f	Normal	L mesial temp	21	21		na
25	39/m	Normal	L mesial temp	13	27		L temp/norm/I/24

Age/sex age at examination/sex, *f* female, *m* male, *MTS* mesial temporal sclerosis at 1.5 T, *Norm* normal MRI at 1.5 T, *R* right, *L* left, *temp* temporal, *WMH* white matter hyperintensities, *Onset* age at onset, *Duration* duration of epilepsy, *FS* febrile seizure, *Infection* history of encephalitis/meningitis without temporal relationship to onset of seizures, *perinatal* perinatal complications, *posttrauma* mild closed head trauma in history without temporal relationship to onset of seizures, *histo* histology, *surgery* epilepsy surgery, *na* no. surgery, *Outcome* latest outcome using Engel's classification is given in roman numerals, follow-up in months is given in arabic numerals

Postprocessing

EPSI postprocessing

A B0 map was derived from the water reference image. The water reference data was then zero-filled from $50 \times 50 \times 18$ to $64 \times 64 \times 24$ points, and a spatial apodization using a Gaussian filter was applied before performing of a four-dimensional spectral FT and B0 correction [18]. The resulting image was used to generate a brain mask which was applied to the metabolite data to avoid fitting of regions of no interest. The metabolite data was corrected for chemical shift artifact, echo averaged and the residual water signal was reduced by applying a finite impulse response (FIR) filter. Spectral processing of the metabolite data included zero filling to 512 points, lipid *k*-space extrapolation and Gaussian apodization with a line broadening of 2 Hz before performing a four-dimensional

FT and spectral fitting with SITOOLS [19] (cf. Fig. 1). A binary map containing only voxels of acceptable quality (QC map) was generated using linewidth (between 3–21.3 Hz) and fit accuracy (fits with residual sum squares outside the 95 percentile distribution of residuals from all fits were rejected) [18, 20] as main criteria. Intensity images for each metabolite of interest (NAA, Cr and Cho) were derived from the fitted metabolite data and used to calculate NAA/(Cr+Cho) maps. NAA/(Cr+Cho) has been found to be very sensitive to the type of metabolic abnormality observed in TLE [13] and has (compared to single metabolite maps) the additional advantage that it does not require an intensity non uniformity correction of the spectral data. Voxels with NAA/(Cr+Cho) >4 indicating an insufficient suppression/extraction of the skull lipid signal were excluded. The final QC map was applied to the resulting ratio map to eliminate spectra with insufficient quality.

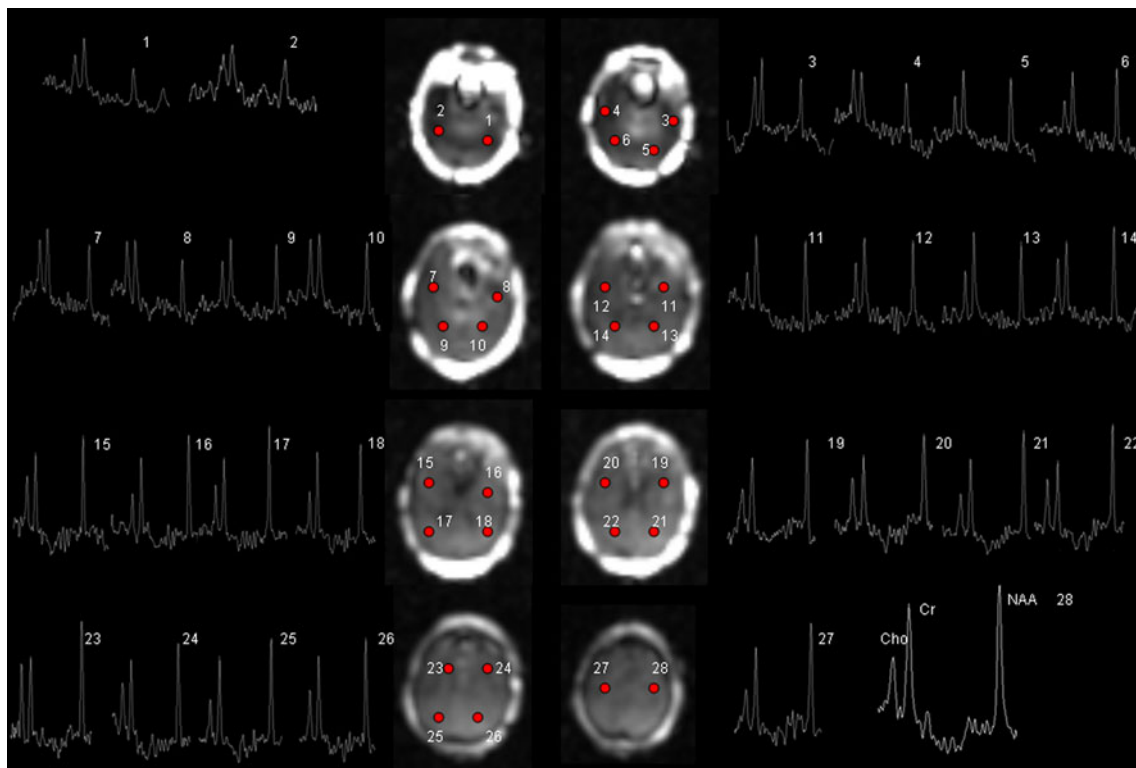


Fig. 1 Raw 3D EPSI with representative spectra from a TLE-MTS patient with a right sided focus. All displayed spectra passed the automated quality control. Spectrum 28 has been enlarged and the

peaks of the main metabolites are labelled. NAA *N*-acetyl-aspartate, Cr creatine/phosphocreatine, Cho choline compounds

Structural image processing

All T1 images were segmented in gray, white and CSF tissue maps using expectation maximization segmentation (EMS) [21, 22].

Combination of structural and EPSI data

The T1 images were co-registered (six affine, mutual information [23]), down-sampled to the resolution of the EPSI water reference image and the resulting transformation matrices were applied to the T1 image and the gray matter map. The resulting down-sampled gray matter maps were spatially normalized to a previously generated customized symmetrical gray matter prior in ICBM (International Consortium for Brain Mapping) space using the spatial normalization algorithm in statistical parametric mapping 2 (SPM2) (Wellcome Department of Cognitive Neurology, <http://www.fil.ion.ucl.ac.uk>) running MATLAB 6.1 (The MathWorks, Natick, MA, USA). The resulting transformations were then applied to the NAA/(Cr+Cho) map with and without QC, the QC map, the T1 image co-registered to the EPSI and the gray matter map. The resulting spatially normalized maps were re-sampled to a $1 \times 1 \times 1$ mm resolution.

Data analysis

Two approaches were used for data analysis: (1) Group analysis: each TLE subgroup was compared to the control group and with each other to identify regions with decreased NAA/(Cr+Cho). In order to allow for the combination of left and right onset TLE patients, the NAA/(Cr+Cho) maps of all right TLE were side flipped so that the hemisphere with the epileptogenic focus was on the left side in all patients. To account for physiological right/left hemispheric differences, all control NAA/(Cr+Cho) maps were also side-flipped and both versions were used for the group comparisons. (2) Single subject analysis: each individual TLE subject was compared to the control group and a map with regions of significantly reduced NAA/(Cr+Cho) generated using SPM2.

Statistical analysis

Group analysis

SPM2 was used to identify regions with significantly decreased NAA/(Cr+Cho) in TLE-MTS compared to controls, in TLE-no compared to controls, and in TLE-MTS compared to TLE-no (compare populations:1 scan/

subject (ANCOVA), age as nuisance variable, threshold for significance at voxel level $p < 0.001$ and $p < 0.05$ corrected at cluster level).

Single subject analysis

SPM2 was used to localize regions of metabolic abnormalities in individual TLE subjects by performing a t test in which each TLE subject was compared with all control subjects [compare populations: 1 scan/subject (two-sample t test)]. The threshold for statistical significance was defined as $p < 0.005$ at voxel level and $p < 0.05$ at cluster level. These thresholds had been determined empirically by comparing each control with all remaining controls and then choosing the threshold at which none of the controls except one had clusters with abnormally low NAA/(Cr+Cho). In this control, these clusters persisted even when higher thresholds (FDR $p < 0.05$) were applied. The localization of each cluster was based on the coordinates of the voxel with the maximal t value. The region with the largest cluster of significantly reduced NAA/(Cr+Cho) was arbitrarily determined to represent the “focus as determined by 3D EPSI”. If the “focus as determined by 3D EPSI” was concordant with the epileptogenic temporal lobe as identified by VET, the EPSI focus identification was considered to be “correct”. EPSI identification of the epileptogenic temporal lobe instead of the hippocampus was chosen because the spectral quality in the hippocampus was often adversely affected by the susceptibility artifacts typical for the basal temporal lobe. This resulted in the loss of the spectra from the head and anterior two-thirds of the body of the hippocampus (on average $26 \pm 14\%$ of the hippocampal voxels fulfilled the quality criteria), i.e., the region where previous studies had shown the most prominent abnormalities in TLE [11]. Because of this, spectral information from the hippocampal tail was lumped together with the temporal lobe for “focus determination by EPSI”. Mann–Whitney tests and Fisher’s exact test were used to compare indices of epilepsy severity and EPSI brain coverage between TLE with and without clusters of abnormally low NAA/(Cr+Cho). Holms’ test was used to correct for multiple comparisons.

Results

Group analysis

Figure 2 displays the results of the group analysis. NAA/(Cr+Cho) abnormalities in TLE-MTS had a bilateral temporo-occipital distribution. Additional prominent abnormalities were present in both frontal lobes. NAA/(Cr+Cho) abnormalities in TLE-no were more diffuse and

less well-defined and were most prominent in the temporo-insular and bilateral frontal regions. The direct comparisons between TLE-MTS and TLE-no showed no significant differences at the chosen significance threshold.

Single subject analysis

Figure 3 displays the results of the single subject analysis for two typical TLE-MTS and two typical TLE-no. Table 2 shows the results for each subject. Three TLE-MTS and five TLE-no had no clusters with significant NAA/(Cr+Cho) reductions. The remaining nine TLE-MTS had 1–5 clusters with abnormally low NAA/(Cr+Cho) [average number (No) of clusters: 2.7; median cluster size: 93,021 (range 1,193–602,663 voxels; median size of largest cluster: 4,515 (range 1,193–5,85,555 voxels)], and the remaining eight TLE-no had 1–7 clusters with abnormally low NAA/(Cr+Cho) [average No of clusters: 4.0; median cluster size: 11,287 (range 1,638–49,841) voxels; median size of largest cluster: 4,828 (range 1,638–26,961 voxels)]. TLE-MTS and TLE-no did not differ from each other regarding number of abnormal NAA/(Cr+Cho) clusters nor regarding the size of these clusters or size of the largest cluster.

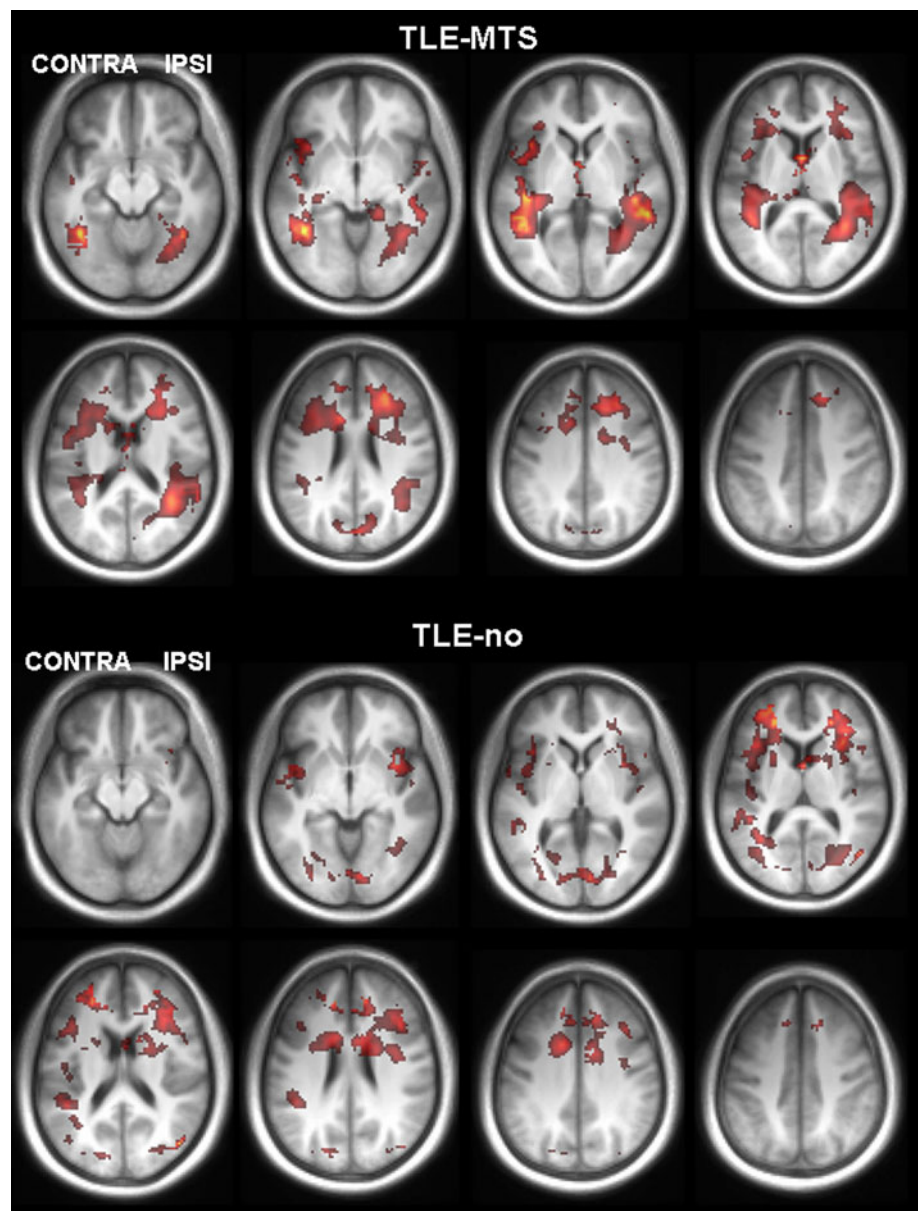
The largest cluster of abnormally low NAA/(Cr+Cho) was in the ipsilateral temporal lobe in five TLE-MTS. In the remaining four TLE-MTS, the largest cluster with abnormally low NAA/(Cr+Cho) was either in the contralateral temporal lobe ($n = 3$) or contralateral ($n = 1$) frontal lobe. In seven TLE-no the largest cluster with abnormally low NAA/(Cr+Cho) was found in the contralateral hemisphere (frontal: 3; insula: 2; parietal: 1, temporal: 1) and in one it was found in the ipsilateral occipital lobe.

Temporal lobe epilepsy with abnormally low NAA/(Cr+Cho) did not differ from TLE with NAA/(Cr+Cho) within the normal range regarding mean duration of epilepsy (22.3 ± 17.5 vs. 20.3 ± 10.9 years, $p = 0.74$), age at onset of epilepsy (19.5 ± 13.8 vs. 18.0 ± 13.5) occurrence of secondary generalized seizures (23.5 vs. 12.5%, $p = 0.47$), occurrence of risk factors for epilepsy (35.3 vs. 37.5%, $p = 0.71$), seizures/month (7.5 ± 15.3 vs. 11.9 ± 14.8 , $p = 0.52$) or % brain coverage by 3DEPSI (35.1 ± 8.2 vs. $39.3 \pm 4.3\%$, $p = 0.19$).

Discussion

There were three major findings in this study: (1) Ipsi- and contralateral temporal and extratemporal regions with abnormally low NAA/(Cr+Cho) were found in TLE-MTS and TLE-no. The extent of these NAA/(Cr+Cho) reductions varied between subjects even within the same

Fig. 2 Regions with significant decreased NAA/(Cr+Cho) in TLE-MTS compared to controls (upper two panels) and TLE-no compared to controls (lower two panels). Abnormalities in TLE-MTS were most prominent in the bilateral temporal lobes but extended also into posterior occipital and frontal regions. Abnormalities in TLE-no were more diffuse, less distinct and preferentially in bilateral frontal, temporal-insular regions. Similarly, as in the single subject analysis, there was no clear predominance of the NAA/(Cr+Cho) reductions in the ipsilateral hemisphere in either group



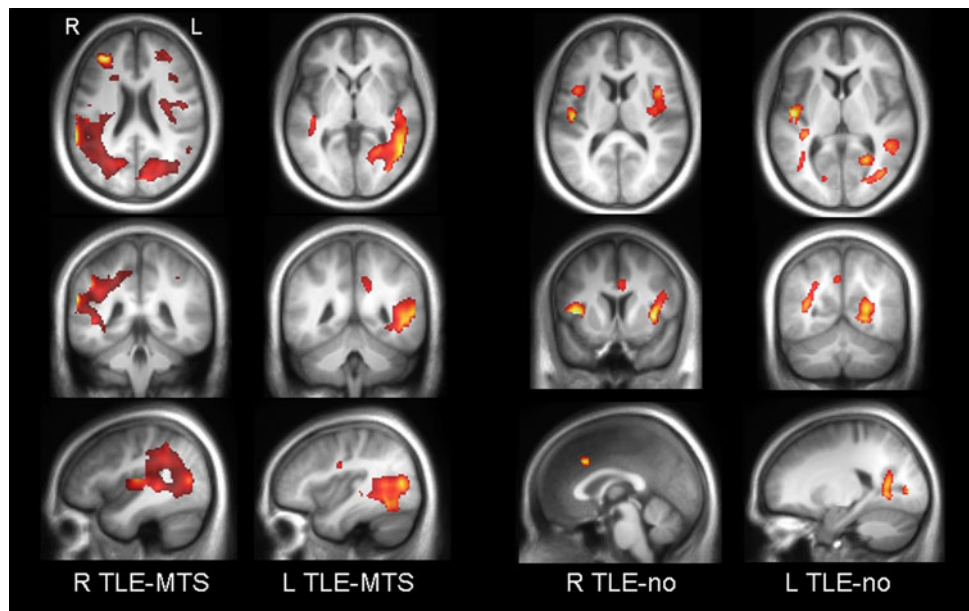
subgroup. Factors that might influence the expression of these abnormalities, e.g., seizure frequency, type, were not different between TLE with and without widespread NAA/(Cr+Cho) reductions. (2) The high degree of interindividual heterogeneity and variability of the metabolic abnormalities complicated the identification of a distinct pattern of NAA/(Cr+Cho) reductions in each of the two TLE subgroups. Although the visual inspection of the TLE vs. control comparisons suggested a predominantly temporal-frontal distribution of the NAA/(Cr+Cho) decreases in TLE-MTS and a more diffuse, less distinct distribution in TLE-no (cf. Fig. 2), the two TLE groups were not significantly different from each other in the direct comparison. (3) Extrafocal NAA/(Cr+Cho) abnormalities did not provide additional information for focus lateralization in

TLE-MTS or in TLE-no. Taken together, this study provides evidence that at least metabolically non-lesional TLE is neither a focal nor a homogeneous disease.

Etiology of extrafocal NAA/(Cr+Cho) reductions

The first finding of this study was the confirmation of the widespread, bilateral extrafocal NAA/(Cr+Cho) reductions in TLE-MTS and TLE-no which had been described by previous spectroscopic imaging studies with partial brain coverage [12, 13]. The etiology of these extrahippocampal NAA/(Cr+Cho) reductions in TLE is unknown. NAA decreases in the hippocampus are usually thought to be caused by neuron loss and/or neuronal dysfunction [9]. The fact that hippocampal NAA decreases have been found to

Fig. 3 Representative results of the single subject analysis. The two TLE-MTS had large ipsilateral temporal clusters which extended in neighboring regions. There were also smaller clusters in the frontal lobes. The two TLE-no in general had smaller and more diffusely distributed clusters



be useful for focus lateralization in TLE [24] suggests that they are stable over time, at least in the epileptogenic hippocampus. Neuronal loss and neuronal dysfunction could also explain the extrahippocampal and extratemporal NAA/(Cr+Cho) reductions found in this study. In analogy to the focus, local excitotoxic effects of spreading epileptogenic activity could lead to neuronal loss in extrafocal regions. In that case it could be expected that the resulting NAA/(Cr+Cho) abnormalities are associated with structural abnormalities/volume loss. Widespread cortical thinning in TLE-MTS and TLE-no with a similar distribution as the NAA/(Cr+Cho) reductions described here has indeed recently been demonstrated in a study from this lab [16]. Extrafocal neuronal dysfunction could be caused by deafferentation due to loss of input from the focus, or by excitotoxic effects of seizure spread too mild to result in neuronal loss. The best evidence that NAA/(Cr+Cho) reductions due to neuronal dysfunction exist in TLE comes from the observation that reduced NAA in the contralateral hippocampus often returns to normal levels after successful surgery [25, 26]. However, the observation that some of the extrafocal NAA/(Cr+Cho) abnormalities are reversible also indicates that the severity and extent of these NAA/(Cr+Cho) reductions are not necessarily stable over time. Longitudinal studies correlating extrahippocampal/extratemporal NAA/(Cr+Cho) changes with structural abnormalities and clinical variables, such as seizure frequency between exams, will be necessary to explore in which regions extrafocal NAA/(Cr+Cho) reductions are stable over time and correspond to an irreversible neuron loss, and in which regions they fluctuate and indicate neuronal dysfunction.

High intersubject variability of NAA/(Cr+Cho) reductions in TLE-MTS and TLE-no

The single subject analysis showed a wide range of these extrafocal NAA/(Cr+Cho) reductions even within the same TLE group with some being metabolically completely normal while others had severe, widespread abnormalities. The high degree of intersubject variability of NAA/(Cr+Cho) abnormalities and the relatively small population sizes made it difficult to identify a distinct pattern of metabolic abnormalities in each of the TLE-subgroups (cf. Fig. 2). The most obvious explanation for the variability of NAA/(Cr+Cho) reductions between patients would be differences in severity and duration of the epileptic disorder. Several studies have described a relationship between structural abnormalities and duration of epilepsy [27, 28]. Therefore, it could be expected that TLE patients with a longer duration of epilepsy, more frequent and/or more severe seizures (occurrence of secondary generalized seizures) have more severe NAA/(Cr+Cho) reductions than subjects with less frequent and/or milder seizures or who developed seizures later in life. However, the direct comparison of metabolically normal TLE with metabolically abnormal TLE provided no evidence that any of these factors had an influence on the severity of the NAA/(Cr+Cho) reductions. Technical issues which could have caused such variations artificially, i.e., differences in % brain coverage between metabolically normal and abnormal subjects resulting in the exclusion of regions with reduced NAA/(Cr+Cho) in the former but inclusion in the latter, also seem unlikely since % brain coverage was not different between subjects with normal

Table 2 Results of single subject analysis

Pat no.	Group	No. cluster	Size cluster	Side	Lobe
1	MTS	0	0	na	na
2	MTS	2	4,515	Contra	Frontal
			2,081	IPSI	Temporal
3	MTS	5	35,365	IPSI	Temporal
			2,258	Contra	Temporal
			1,408	IPSI	Frontal
			2,342	Contra	Frontal
			1,420	IPSI	Parietal
4	MTS	1	1,193	Contra	Temporal
5	MTS	1	1,652	Contra	Temporal
6	MTS	0	0	na	na
7	MTS	5	9,708	IPSI	Frontal
			97,853	IPSI	Temporal
			12,774	Contra	Frontal
			1,784	Contra	Temporal
			5,487	Contra	Frontal
8	MTS	1	1,295	IPSI	Temporal
9	MTS	1	2,481	Contra	Temporal
10	MTS	4	15,170	Contra	Frontal
			21,965	IPSI	Temporal
			3,773	Contra	Temporal
			10,002	Contra	Parietal
11	MTS	4	6,609	IPSI	Frontal
			1,350	Contra	Frontal
			585,555	IPSI	Temporal
			9,149	Contra	Temporal
12	MTS	0	0	na	na
13	Norm	7	2,966	Contra	Insula
			1,147	Contra	Temporal
			1,303	IPSI	Frontal
			7,799	Contra	Parietal
			6,211	IPSI	Occipital
			1,326	Contra	Frontal
			2,239	IPSI	Temporal
14	Norm	1	1,638	Contra	Insula
15	Norm	0	0	na	na
16	Norm	5	1,740	Contra	Occipital
			1,792	Contra	Frontal
			1,269	IPSI	Frontal
			1,257	Contra	Temporal
			1,587	IPSI	Occipital
17	Norm	4	6,625	Contra	Insula
			2,062	IPSI	Insula
			2,625	IPSI	Frontal
			3,121	Bi	Frontal
18	Norm	0	0	na	Na

Table 2 continued

Pat no.	Group	No. cluster	Size cluster	Side	Lobe
19	Norm	3	2,518	IPSI	Frontal
			2,708	Contra	Parietal
			2,915	Contra	Frontal
20	Norm	0	0	na	Na
21	Norm	4	2,532	IPSI	Frontal
			5,813	Contra	Occipital
			7,243	Contra	Frontal
			1,365	IPSI	Temporal
22	Norm	1	3,030	IPSI	Occipital
23	Norm	7	2,400	Contra	Frontal
			18,384	IPSI	Occipital
			3,983	Contra	Frontal
			18,552	Contra	Temporal
			3,102	Bi	Frontal
			2,228	Bi	Frontal
			1,192	IPSI	Frontal
24	Norm	0	0	na	na
25	Norm	0	0	na	na

IPS ipsilateral, *Contra* contralateral, *Bi* bilateral, *MTS* mesial temporal sclerosis, *Norm* normal, *No. cluster* number of clusters, *Size cluster* number of voxels with abnormally low NAA/(Cr+Cho) in the cluster, *bold* cluster which fulfill criterion for “focus as identified by EPSI” and are concordant with EEG identification of the focus

EPSI and those with abnormal EPSI. There are, of course, a multitude of other potential factors which alone or in combination might explain the wide range of NAA/(Cr+Cho) abnormalities observed in non-lesional TLE, e.g., interval between last seizure and scan [29], type of the last seizure [30], type of antiepileptic medication, different individual vulnerability for effects of epileptogenic activity in non epileptogenic brain tissue, etc. Longitudinal studies in a larger patient population might help to identify the factors contributing to this variability.

Value of extrafocal NAA/(Cr+Cho) reductions for focus lateralization

The lateralizing information provided by NAA/(Cr+Cho) reductions in individual TLE-MTS patients was minimal. Only 42% of the TLE-MTS had the largest cluster of reduced NAA/(Cr+Cho) in the ipsilateral temporal lobe and the hemispheric NAA/(Cr+Cho) reductions were not significantly different between the ipsi- and contralateral hemispheres. The lateralizing information was even worse for TLE-no. There were no significant ipsi-/contralateral hemispheric differences and the largest cluster of low

NAA/(Cr+Cho) were in all cases extratemporal. Based on this, it can be concluded that extrahippocampal/extratemporal NAA/(Cr+Cho) reductions do not provide additional information for focus lateralization. Further study will be needed to address the question if the extent and distribution of these extrafocal NAA/(Cr+Cho) reductions might be useful to predict post-surgical seizure control or cognitive impairment.

Technical limitations

The study has limitations: (1) Loss of spectral data affected particularly the basal and mesial temporal lobe, i.e., regions which are prominently affected in TLE. Therefore, we may have missed significant temporal NAA/(Cr+Cho) reductions providing lateralizing information. This might also explain why four patients (Pat No 4, 5, 9, 14) had only contralateral abnormalities. Future studies should combine 3D EPSI with a single slice hippocampal measurement to ensure that data is also consistently collected from these regions. (2) For the reasons outlined in the methodological sections, we used NAA/(Cr+Cho) maps and not single metabolite maps. Therefore, we cannot exclude that some of the metabolic abnormalities were caused by elevated Cho and/or Cr concentrations rather than by NAA decreases. (3) The study population was small and so lack of statistical power might be responsible for some of the negative findings, e.g., such as not finding significant ipsi-/contralateral differences. (4) All patients were recruited from tertiary care centers where they were evaluated for epilepsy surgery. These patients were probably suffering from a more severe form of TLE and, thus, may not be representative for non-lesional TLE in general. It will therefore be necessary to replicate the findings in a larger, more diverse TLE population. In addition to duration of epilepsy, seizure frequency, etc., future studies should also address the influence of other factors on extrafocal NAA/(Cr+Cho) reductions, e.g., contribution of antiepileptic treatment, correlation with extent of EEG abnormalities.

Conclusion

This study confirmed the findings of previous spectroscopic imaging studies which demonstrated wide spread extrafocal NAA/(Cr+Cho) abnormalities in TLE-MTS and TLE-no. The finding that extrafocal NAA/(Cr+Cho) reductions show a considerable individual variation in extent and severity within each of the subtypes demonstrates that a homogeneous pattern of neuronal dysfunction/neuronal loss does not exist in either TLE-MTS or TLE-no. Further studies will be necessary to obtain a better understanding of the nature of these metabolic abnormalities and of their

influence on cognitive performance and long term outcome after epilepsy surgery.

Acknowledgments This work was supported by the National Institute of Health grant RO1-NS31966 to K.D.L. None of the authors has any conflict of interest to disclose.

Open Access This article is distributed under the terms of the Creative Commons Attribution Noncommercial License which permits any noncommercial use, distribution, and reproduction in any medium, provided the original author(s) and source are credited.

References

1. Carne RP, Cook MJ, MacGregor LR, Kilpatrick CJ, Hicks RJ, O'Brien TJ (2007) Magnetic resonance imaging negative positron emission tomography positive temporal lobe epilepsy: FDG-PET pattern differs from mesial temporal lobe epilepsy. *Mol Imaging Biol* 9:32–42
2. Mueller SG, Laxer KD, Schuff N, Weiner MW (2007) Voxel-based T2 relaxation rate measurements in temporal lobe epilepsy (TLE) with and without mesial temporal sclerosis. *Epilepsia* 48:220–280
3. Bernasconi N, Bernasconi A, Caramanos Z, Dubeau F, Richardson J, Andermann F, Arnold DL (2001) Entorhinal cortex atrophy in epilepsy patients exhibiting normal hippocampal volumes. *Neurology* 56:1335–1339
4. Keller SS, Roberts N (2008) Voxel-based morphometry of temporal lobe epilepsy: an introduction and review of the literature. *Epilepsia* 49:741–757
5. Bernhardt BC, Worsley KJ, Besson P, Concha L, Lerch JL, Evans AC, Bernasconi N (2008) Mapping limbic network organization in temporal lobe epilepsy using morphometric correlations: insights on the relation between mesiotemporal connectivity and cortical atrophy. *Neuroimage* 42:515–524
6. Vossler DG, Kramer DL, Haltiner AM, Rostad SW, Kjos BO, Davis BJ, Moran JD, Caylor LM (2004) Intracranial EEG in temporal lobe epilepsy: location of seizure onset relates to degree of hippocampal pathology. *Epilepsia* 45:450–497
7. Cohen-Gadol AA, Bradley CC, Williamson A, Kim JH, Westerveld M, Duckrow RB, Spencer DD (2005) Normal magnetic resonance imaging and medial temporal lobe epilepsy: the clinical syndrome of paradoxical temporal lobe epilepsy. *J Neurosurg* 102:902–909
8. Bell ML, Rao S, So EL, Trenerry M, Kazemi N, Stead SM, Cascino G, Marsh R, Meyer B, Watson RE, Giannini C, Worrell GA (2009) Epilepsy surgery outcome in temporal lobe epilepsy with a normal MRI. *Epilepsia* 50:2053–2060
9. Cohen-Gadol AA, Pan JW, Kim JH, Spencer DD, Hetherington HH (2004) Mesial temporal lobe epilepsy: a proton magnetic resonance spectroscopy study and histopathological analysis. *J Neurosurg* 101:613–620
10. Hammen T, Hildebrandt M, Stadlbauer A, Engelhorn T, Doelken M, Kerling F, Kaspar B, Romstoeck J, Ganslandt O, Nimsky C, Blumcke I, Doerfler A, Stefan H (2008) Non-invasive detection of hippocampal sclerosis: correlation between metabolite alterations detected by (1)H-MRS and neuropathology. *NMR Biomed* 21:545–552
11. Vermathen P, Laxer KD, Matson GB, Weiner MW (2000) Hippocampal structures: anteroposterior *N*-acetylaspartate differences in patients with epilepsy and control subjects as shown with proton MR spectroscopic imaging. *Radiology* 214:403–410

12. Capizzano AA, Vermathen P, Laxer KD, Matson GB, Maudsley AA, Soher BJ, Schuff N, Weiner MW (2002) Multisection proton MR spectroscopy for mesial temporal lobe epilepsy. *Am J Neuroradiol* 23:1359–1368
13. Mueller SG, Laxer KD, Cashdollar N, Flenniken DL, Matson GB, Weiner MW (2004) Identification of abnormal neuronal metabolism outside the seizure focus in temporal lobe epilepsy. *Epilepsia* 45:355–366
14. Maudsley AA, Domenig C, Ramsay RE, Bowen BC (2010) Application of volumetric MR spectroscopic imaging for localization of neocortical epilepsy. *Epilepsy Res* 88:127–138
15. Ebel A, Maudsley AA (2003) Improved spectral quality for 3D MR spectroscopic imaging using a high spatial resolution acquisition strategy. *Magn Reson Imaging* 21:113–120
16. Mueller SG, Laxer KD, Barakos J, Cheong I, Garcia P, Weiner MW (2009) Widespread neocortical abnormalities in temporal lobe epilepsy with and without mesial temporal sclerosis. *Neuroimage* 46:353–359
17. Mueller SG, Laxer KD, Barakos J, Cheong I, Garcia P, Weiner MW (2009) Subfield atrophy pattern in temporal lobe epilepsy with and without mesial sclerosis detected by high resolution MRI at 4 Tesla: preliminary results. *Epilepsia* 50:1474–1483
18. Ebel A, Maudsley AA, Schuff N (2007) Correction of local B0 shifts in 3D EPSI of the human brain at 4T. *Magn Reson Imaging* 25:377–380
19. Soher BJ, Young K, Govindaraju V, Maudsley AA (1998) Automated spectral analysis III: application to in vivo proton spectroscopy and spectroscopic imaging. *Magn Reson Med* 40:822–831
20. Ebel A, Soher BJ, Maudsley AA (2001) Assessment of 3D proton MR echo-planar spectroscopic imaging using automated spectral analysis. *Magn Reson Med* 46:1072–1078
21. Van Leemput K, Maes F, Vandermeulen D, Suetens P (1999) Automated model-based bias field correction of MR images of the brain. *IEEE Trans Med Imaging* 18:885–896
22. Van Leemput K, Maes F, Vandermeulen D, Suetens P (1999) Automated model-based tissue classification of MR images of the brain. *IEEE Trans Med Imaging* 18:897–908
23. Studholme C, Hill DL, Hawkes DJ (1996) Automated 3-D registration of MR and CT images of the head. *Med Image Anal* 1:163–175
24. Connelly A, Jackson GD, Duncan JS, King MD, Gadian DG (1994) Magnetic resonance spectroscopy in temporal lobe epilepsy. *Neurology* 44:1411–1417
25. Simister RJ, McLean MA, Barker GJ, Duncan JS (2009) Proton MR spectroscopy of metabolite concentrations in temporal lobe epilepsy and effect of temporal lobe resection. *Epilepsy Res* 83:168–176
26. Serles W, Li LM, Antel SB, Cendes F, Gotman J, Olivier A, Andermann F, Dubeau F, Arnold DL (2001) Time course of postoperative recovery of *N*-acetyl-aspartate in temporal lobe epilepsy. *Epilepsia* 42:190–197
27. McDonald CR, Hagler D, Ahmadi ME, Tecoma E, Iragui V, Gharapetian L, Dale AM, Halgren E (2008) Regional neocortical thinning in mesial temporal lobe epilepsy. *Epilepsia* 49:794–803
28. Coan A, Appenzeller S, Bonilha L, Li LM, Cendes F (2009) Seizure frequency and lateralization affect progression of atrophy in temporal lobe epilepsy. *Neurology* 73:834–842
29. Simister RJ, McLean MA, Salmenpera TM, Barjer GJ, Duncan JS (2008) The effect of epileptic seizures on proton MRS visible neurochemical concentrations. *Epilepsy Res* 81:36–43
30. Savic I, Altshuler L, Baxter L, Engel J (1997) Pattern of interictal hypometabolism in PET scans with fludeoxyglucose F18 reflects prior seizure types in patients with mesial temporal lobe seizures. *Arch Neurol* 54:129–136